A critical steel yielding length model for predicting intermediate crack-induced debonding in FRP -strengthened RC members

Jian-Guo Dai*

*Department of Civil and Structural Engineering, The Hong Kong Polytechnic University
Hung Hom, Kowloon, Hong Kong*

Kent A. Harries

*Department of Civil and Environmental Engineering, University of Pittsburgh
936 Benedum Hall, Pittsburgh PA 15261, U.S.A*

Hiroshi Yokota

Port and Airport Research Institute, Yokosuka 239-0826, Japan

Abstract. Yielding of the internal steel reinforcement is an important mechanism that influences the Intermediate Crack-induced debonding (IC debonding) behavior in FRP-strengthened RC members since the FRP is required to carry additional forces beyond the condition of steel yielding. However, rational design practice dictates an appropriate limit state is defined when steel yielding is assured prior to FRP debonding. This paper proposes a criterion which correlates the occurrence of IC debonding to the formulation of a critical steel yielding length. Once this length is exceeded the average bond stress in the FRP/concrete interface exceeds its threshold value, which proves to correlate with the average bond resistance in an FRP/concrete joint under simple shear loading. This proposed IC debonding concept is based on traditional sections analysis which is conventionally applied in design practice. Hence complex bond stress-slip analyses are avoided. Furthermore, the proposed model incorporates not only the bond properties of FRP/concrete interface but also the beam geometry, and properties of steel and FRP reinforcement in the analysis of IC debonding strength. Based upon a solid database, the validity of the proposed simple IC debonding criterion is demonstrated.

1. Introduction

Using externally bonded FRP sheets/laminates to strengthen reinforced concrete (RC) beams in flexure has become relatively commonplace. Since the early 1990s, numerous experimental tests have demonstrated the efficiency of this strengthening technique in terms of both strength and stiffness

---

*Corresponding Author, E-mail: cejgdai@polyu.edu.hk

enhancement (Saadatmanesh and Ehsani 1991, Triantafillou and Plevris 1992, Meier 1995, Arduini *et al*. 1997, Garden *et al*. 1998, Kim and Aboutaha, 2004). However, a major concern for FRP flexural strengthening is the premature debonding between FRP and concrete substrate occurring along the bonded interface: the weakest link in the whole strengthening system. As has been well documented (Buyukozturk and Hearing 1998, Triantafillou 1999, Sebastian 2001, Teng *et al*. 2002, Oehlers 2005), two primary debonding mechanisms are widely observed. One is the plate-end debonding initiating from the termination point of FRP. The main factors causing this failure are understood to be the distance between the termination positions of the FRP and the beam supports (in simple spans) and the use of thick FRP plates. In practice, this failure can be mitigated by extending the FRP as near as possible to the beam supports (or beyond the point of inflection) or by installing U-shape anchorage systems at the FRP ends to resist peeling (Mode I) forces. The second debonding mechanism is Intermediate Crack-Induced debonding (IC debonding) caused by the opening of major flexural and flexure-shear cracks (Oehlers 2005, Teng *et al*. 2003). Since the IC debonding is the most prevalent failure mode in FRP-strengthened RC flexural members and is not easily mitigated by mechanical means, design codes (ACI 2002, JSCE 2001, FIB 2001) have specified methods to predict the member strength corresponding to this limit state. Recently, efforts have been put into predicting the full-range debonding processes along the length of cracked concrete beams using crack spacing and functions describing the bond-slip behavior of the FRP/concrete interface. Except for a few models developed based on a fracture mechanics approach [Gunes 2006, Achintha and Burgoyne 2006], other models developed for predicting the IC debonding in FRP-strengthened flexural RC members can be sorted into the following two types:

  (1) Strain limit-based approach. The concept for this approach is to limit the strain/stress in the externally bonded FRP to below a threshold level. In the FIB 2001 code, the strain in FRP is limited to less than five times the steel yielding strain or half of the characteristic values of the ultimate strain of the FRP according to the manufacturer. The ACI 440 (2002) code correlates the strain limit to the tension stiffness of FRP. Forthcoming revisions of the ACI 440 code adopt the Teng *et al*. (2003) approach to debonding (although with different calibration factors) which additionally addresses concrete substrate behavior. The debonding strain in FRP has also been correlated with other factors such as the fracture energy of FRP/concrete interface (JSCE 2001), concrete strength, the ratio of FRP width to concrete surface width (Teng *et al*. 2003), bond length of FRP, the effective bond length of FRP/concrete interface, and the maximum interfacial bond stress (Lu *et al*. 2007). Such strain limit models derived from various approaches are preferred in design practice. However, their reliability is questioned since they reflect the influences of FRP properties and the interface bond while generally neglecting information such as the beam geometry and internal reinforcement ratio. Leung *et al*. (2006) applied a neural network approach to analyze an experimental database of 143 tests and showed that it is necessary to consider the effects of beam geometry such as the shear span/depth ratio, concrete cover depth etc. for developing a debonding strain model.

  (2) Stress variation-based approach. In this approach, the distribution of cracks in an FRP-strengthened flexural RC beam is considered and the bond stress-slip relationship for the FRP sheet/concrete interface is necessary to implement an analysis. For strengthened members having a single flexural crack, the debonding strength analysis is not complex. Closed-form solutions for FRP delamination in the case of a single flexural crack case are presented by Leung (2006) based on a linear analytical approach and Wang (2006) based on a non-linear approach. Extensive studies have shown that the stress condition at an interface having a single flexural crack is similar to that of the simple pull-out shear test (Wu and Niu 2000, Leung and Tung 2006, and Liu *et al*. 2007). Therefore, the debonding stress in FRP can be determined using the Mode II fracture energy of FRP/concrete interfaces (Holzenkämfer

1994, Täljsten 1996, Brosens and Van Gemert 1998, Chen *et al*. 2001). The single flexural crack case is described by Oehlers (2005) as "VAy/Ib debonding" (referring to the interface shear calculated in this manner). Oehlers correctly points out that VAy/Ib debonding will not be a controlling limit state in an element where there exists a cracked region having a moment gradient. This type of debonding may become relevant however for prestressed beams where flexural cracks are suppressed or for serviceability-retrofits where thick plates may be used to control deflections when there are few flexural cracks.

For practical cases in which multiple cracks exist in the FRP-strengthened RC members, the IC debonding failure needs to be predicted considering the variation of tensile stresses in the FRP bonded to the concrete "tooth" between adjacent cracks. Early analytical work related to this debonding mechanism can be found in Niedermeier (2000) and Niu and Wu (2001, 2002), which was reflected in the FIB (2001) and JSCE codes (2001), respectively. Recently, continuing efforts have been put into clarifying the variation of tensile stresses in FRP that bridges multiple cracks based on a local deformation model (Smith and Gravina 2007), partial interaction theory (Liu *et al*. 2007), discrete FEM modeling (Niu and Wu 2006), and the application of closed-form solutions (Chen *et al*. 2005, Pan and Leung 2005, Teng *et al*. 2006) using bilinear or tri-linear interfacial bond stress-slip models.

Such stress variation-based approaches are more generic and believed to be superior to existing strain-limit models because they quantitatively clarify the effects of number of cracks, beam geometry, and interface bond properties on the entire interface debonding process. Their complexity, however, is an impediment to developing a practical debonding strength model that unifies all design parameters. Additionally, most of these stress variation-based models are sensitive to the determination of crack-spacing, for which no good models have been proposed for FRP-strengthened RC members. Another issue which remains theoretically controversial is that the debonding strains of FRP are derived from complex bond-slip analysis in which the loss of partial or complete bond action between FRP and one or more cracked concrete "teeth" is allowed at the ultimate limit state. Such derived local FRP strains may better reflect reality. However, when meant for design practice, for which conventional compatibility analysis neglecting the slip between the FRP and concrete is usually applied, their applicability requires further confirmation.

This paper proposes a simple criterion for predicting the IC debonding strength of-FRP strengthened RC beams using the steel yielding phenomenon. Using this simple but useful criterion, all the geometrical information of the strengthened RC beam, its reinforcement details, and the bond properties of the FRP/concrete interface can be incorporated in the IC debonding strength analysis while avoiding complex bond stress-slip analysis or the use of other controversial parameters such as crack spacing, effective bond length, etc.

2. Critical steel yielding length in FRP-strengthened RC members

Failure limit states of FRP-strengthened flexural RC members can be classified into five modes as follows [13]: (1) FRP fracturing following steel yield; (2) Concrete crushing following steel yield; (3) Concrete crushing prior to steel yield; (4) Debonding of FRP at the anchorage zone (so called, end peel); and (5) Mid-span FRP debonding. A conventional compatibility approach can be employed for analyzing the failure mechanisms (1) through (3). The fourth mechanism (4) is related to the stress concentration at the termination point of FRP and is beyond the scope of this paper. The fifth mechanism (5) is the most prevalent failure mode in FRP-strengthened RC beams and is considered in this paper.

The following discussion considers an FRP-strengthened RC beam under three-point bending as

shown in Fig.1. Different from an FRP/concrete joint under simple shear, an FRP-strengthened RC beam under flexure has two important mechanisms influencing the IC debonding between FRP and concrete. The first is the influence of multiple flexure or flexure-shear cracks in the concrete, which has been pointed out by many researchers as reviewed in the previous section. As is shown in Fig. 1, the existence of cracks causes variations of tensile forces in both the FRP and steel reinforcement at cracked and un-cracked sections because of the tension stiffening affected through the bond between concrete and steel and FRP. Good understanding on the local bond stress-slip models for FRP/concrete interfaces helps us to predict these variations and to understand the entire interface debonding process. However, it should be kept in mind that the critical mechanism to cause the macro-debonding failure of an FRP-strengthened system is still the gradient of tensile force in FRP in the shear span (see Fig. 1). This implies a similar debonding behavior in a flexural test and a simple shear test where Mode II interface behavior dominates.

Steel yielding is the second important mechanism influencing IC debonding but has only received limited attention (Ibars 2005, Wu and Niu 2007). As shown in Fig. 1, the tensile force profiles in FRP in the shear span change dramatically before and after steel yielding. This phenomenon is especially easy to observe in large-scale specimens. Fig. 2 presents the strain profiles in the FRP for the strengthening of a bridge deck with a large span (Dai *et al*. 2005a). It can be clearly seen that the strain gradients in FRP behave differently in and out of the steel yielding zone following steel yield. Similar FRP strain profiles within the steel yielding zone can be seen in the FEM analytical results (Niu and Wu 2002, Lu *et al*. 2007). Clearly, the yielding of steel reinforcement not only leads to an increase of local strain in FRP but also leads to an increase of the local strain gradient in FRP. In practice, most FRP-strengthened RC beams are designed with steel yielding at the ultimate state. Hence great interest remains in the possibility of building a direct relationship between the steel yielding and the ultimate IC debonding while avoiding complex analyses based on crack distribution and interfacial bond-slip relationships.

For a simply-supported FRP-strengthened RC beam with steel yielding as shown in Fig. 1, conceptually there is a relationship between the steel yielding length and the ultimate section moment capacity:

$$L_{y,u} = (M_u - M_y)/V_u = (1 - M_y/M_u) \cdot a \tag{1}$$

where $L_{y,u}$ = the steel yielding length in the strengthened member at the ultimate state; M_u = maximum
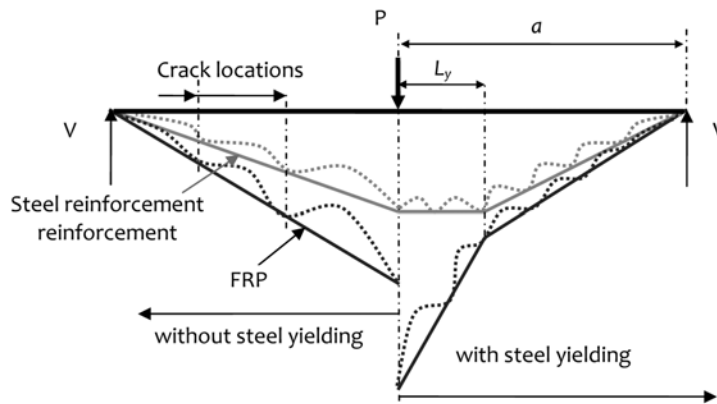

Fig. 1 Difference in tensile stress profile in FRP before and after steel yields
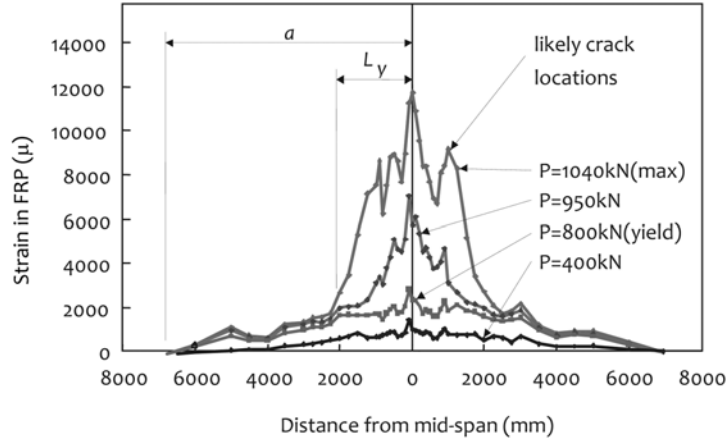
Fig. 2 Strain profiles of FRP in a large-span RC deck strengthened with FRP (Dai *et al*. 2005a)

moment capacity of the strengthened RC member; M_y = maximum moment in the member at initial steel yielding; V_u = shear force in the member at the ultimate state; a = shear span. From Eq.1 it can be seen that the steel yielding length can be a parameter to bridge the ultimate member strength with the beam section geometry (depth, reinforcing ratio, etc.) and shear span. For FRP-strengthened RC beams with debonding failure following steel yield, the debonding strength can be predicted once the length of steel yielding zone at debonding is known.

3. Tensile force variations in FRP driven by steel yielding

Traditional moment-curvature analysis based on plane sections assumption has proved to be applicable for predicting the behavior of FRP-strengthened RC beams (Saadatmanesh and Ehsani 1991). By this method it is not difficult to obtain the tensile force in FRP in the beam section with initial steel yielding. Once the gradient of the tensile force in the FRP, and therefore the average bond stress of FRP/concrete interface within the steel yielding zone is known, the tensile force in FRP at the section with the maximum moment can be obtained as follows:

$$\sigma_{u,frp} = \sigma_{y,frp} + \tau_{aver,u} L_{y,u} / t_{frp} \tag{2}$$

where $\sigma_{u,frp}$ = the maximum tensile force in FRP at the ultimate state; $\sigma_{y,frp}$ = the tensile force in FRP at the beam section with initial steel yielding; $\tau_{aver,u}$ = the average bond stress in the FRP/concrete interface within the steel yielding zone; t_{frp} = the thickness of FRP.

The dotted line in Fig. 3 shows a typical relationship between the average bond stress $\tau_{aver,Ly}$ in the FRP/concrete interface within the steel yielding zone and the steel yielding length L_y, which can be obtained through a traditional sectional analysis. It can be seen that $\tau_{aver,Ly}$ driven by the steel yielding increases with the steel yielding length L_y. Therefore, the occurrence of IC debonding can be attributed to the average bond stress in the steel yielding zone reaching a threshold value beyond which the yielding length can not increase. This threshold value is related to the bond resistance of FRP/concrete interface under shear (Mode II) because, as mentioned above, shear is the mechanism causing the gradient of the
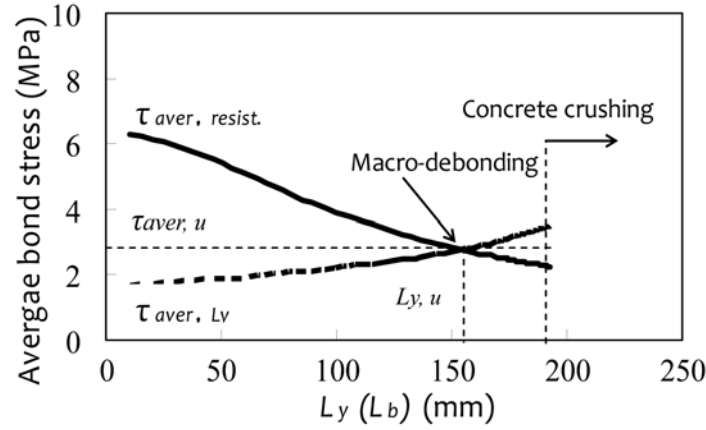
Fig. 3 Typical relationship between the average bond stress in FRP/concrete interface within the yielding zone and the steel yielding length

tensile force in the FRP. In reality, the tension stiffening effect of cracked concrete also influences the localized gradient of the tensile force in the FRP in the vicinity of cracks (see Fig. 1). However, the tension stiffening effects and the localized debonding phenomena due to flexural action are usually understood to be important factors primarily influencing serviceability (Ceroni *et al.* 2004, Ueda *et al.* 2002). It should also be noted that concrete crushing, instead of the IC debonding, will occur if the average bond stress within the yielding zone does not reach its threshold value before the top concrete fiber reaches its ultimate capacity.

4. Bond resistance of FRP/concrete interface under simple shear

Theoretically, for an FRP/concrete joint with a sufficiently long bond length under simple shear (see Fig. 4), the maximum tensile force achieved in FRP can be expressed as:

$$P_{max} = b_f \sqrt{2 E_f t_f G_f} \tag{3}$$

where $G_f =$ is the interfacial fracture energy; E_f, t_f and $b_f =$ the elastic modulus, thickness and width of the FRP, respectively. Dai *et al* (2005b) also proposed a local bond stress-slip relationship for the FRP/ concrete interface as follows:

$$\tau = 2BG_f(e^{-Bs} - e^{-2Bs}) \tag{4}$$

where $\tau =$ local interfacial bond stress; $s =$ local interfacial slip; $B =$ interfacial ductility factor. The interfacial fracture energy G_f and B were found to change greatly when using softer non-linear adhesives. For conventionally used bonding adhesives that behave in a linear manner, Dai *et al.* (2006) suggests the values of G_f and B based on regression analysis of many test results as follows:

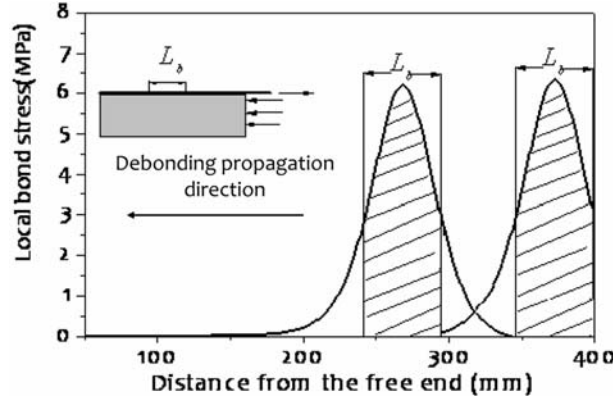$$G_f = 0.514 f_c'^{0.236} \quad \text{(f}_c' \text{ in MPa units)} \tag{5}$$

Fig. 4 Typical shear bond stress distribution in FRP/concrete joints under a simple shear testFig. 5 Stress and strain profiles of FRP-strengthened cross section

$$B = 10.4 \tag{6}$$

Once the interfacial bond-stress slip relationship is known, it is possible to predict the full-range shear bond stress distribution in the FRP/concrete interface under simple shear (see Fig. 4). Using this bond stress distribution, it is also possible to predict the maximum gradient of tensile force in FRP that can be achieved over a given bond length of L_b (see Fig. 4) from the pulled side of FRP using the following formulation:

$$\Delta P_{\max, L_d} = \alpha P_{\max} \tag{7}$$

$$\alpha = (e^{\beta} - 1)/(e^{\beta} + 1) \tag{8}$$

$$\beta = L_b B \sqrt{G_f} / \sqrt{2 E_f t_f} \tag{9}$$

where $\Delta P_{\max, Ld}$ = the maximum gradient of tensile force that can be achieved in a bond area with length L_b. As a consequence, the average bond stress resistance $\tau_{aver, resist.}$ (L_b) over a given bond length, L_b, can be formulated as follows:

$$\tau_{aver, resist} L_b \Delta P_{\max, L_d} / (b_f L_b) = \alpha \sqrt{2 G_f E_f t_f} \tag{10}$$

If the relationship between $\tau_{aver, resist}$ (L_b) and L_b is plotted in Fig. 3, it is seen that $\tau_{aver, resist}$ decreases with the increase of L_b. When L_b approaches 0, mathematically Eq. 10 will converge to the value equal to $0.5G_fB$, whose physical meaning is the maximum local bond stress in the local bond stress-slip relationship (Dai *et al*. 2005b).

5. Proposed IC debonding criterion and verification

Accepting that the primary mechanism leading to macro-debonding is the shear-induced tensile force

gradient in the FRP, it is informative to investigate the relationship between the threshold average bond stress within the steel yielding zone and the average bond resistance of an FRP/concrete interface subject to simple shear. For this purpose, conventional moment-curvature analysis was performed for FRP-strengthened RC members based on a database of 97 tests chosen from 17 sources (refer to Table 2). To have reliable analyses and to achieve the purposes of the current study, the following criteria were applied for selecting test results from the available literature.

(1) All beam geometry information including beam height and width, shear span, effective depth and cover depth was available;

(2) All the reinforcing information including the reinforcing ratio, elastic modulus and yield strength of steel reinforcement, and the elastic modulus, bond width, and thickness of FRP materials was available;

(3) No shear failure was reported for the selected beams/slabs. Also, for the selected simply-supported beams/slabs, the distance between the FRP termination point and the support was sufficiently short to avoid plate-end effects. For this purpose, it was required that the FRP extended over at least 90% of the shear span; and

(4) In the literature, some beams/slabs were reported to have debonding failure. But if they had reported debonding strengths larger than the analytical member strengths corresponding to a concrete crushing failure, they were removed from the database because this condition was considered unrealistic if all the material properties, such as the mechanical properties of FRP and concrete, were correctly reported. Table 1 presents a summary of the range of material and geometry properties of the eventually selected beams/slabs:

An analysis was performed for each FRP-strengthened member based on strain compatibility and force equilibrium (see Fig. 5) conditions. The plane sections assumption was applied and no slip was assumed between FRP and concrete. An elastic-perfectly plastic stress-strain relationship was assumed

Table 1 Summary of material and geometry properties of selected beams/slabs

Test variables	Specimen parameter	Maximum	Minimum	Average
Beam/slab geometry	Depth $h(mm)$	470	100	243
	Width $b(mm)$	800	100	200
	Shear span $a(mm)$	1982.5	340	1024
	Cover depth d'' (mm)	65	15	36
	Shear span/depth ratio a/d	10	2.1	4.7
Tensile reinforcement	Elastic modulus $Es(GPa)$	220	190	206
	Reinforcing ratio $_s$ $(\%)$	1.14	0.33	0.73
	Yielding strength $f_{y,s}$ (MPa)	565	256	406
FRP reinforcement	Elastic modulus (GPa)	271	20.5	173
	Thickness t_{frp} (mm)	6	0.71	0.71
	Tension stiffness $E_{frp}t_{frp}(N/mm)$	308	17.5	99.5
	Width b_{frp} (mm)	200	30	117
	Tensile strength $f_{frp,u}$ (MPa)	4519	269	2742
	Bond length in shear span l_a (mm)	1827.5	320	944.6
	l_α / α	9.95	2.21	4.65
	Strengthening ratio $E_{frp}b_{frp}t_{frp}/(E_sA_s)$	0.69	0.03	0.19
Concrete	Compressive strength f_c' (MPa)	60.8	12.6	33.2

Fig. 5 Stress and strain profiles of FRP-strengthened cross section

for the steel reinforcement and a linear stress-strain behavior was assumed for the FRP to fracture. Hognestad's parabolic stress-strain model was used to describe the constitutive law for concrete in compression (see Fig. 6). The detailed analytical procedures for each strengthened member were as follows:

(1) Calculate the initial yielding moment M_y and the corresponding tensile stress $\sigma_{y, frp}$ in the FRP. Since the experimental maximum moment was known, the steel yielding length $L_{y, u}$ at the ultimate state is calculated using Eq. 1. The maximum tensile stress $\sigma_{u, frp}$ in the FRP at the ultimate state is also obtained;

(2) Using Eq. 2, the average bond stress $\tau_{aver, u}$ within the steel yielding zone is calculated; and

(3) Using Eq. 10, the average bond stress resistance $\tau_{aver, resist}$ over a given bond length L_y under simple shear is determined.

Fig. 7 shows the comparison between $\tau_{aver, u}$ and $\tau_{aver, resist}$. Despite the observed scatter, the correlation of

$$f_c = f_c'\left[1 - \frac{0.15}{0.004 - \varepsilon_0}(\varepsilon_c - \varepsilon_0)\right]$$

$$f_c = f_c'\left[\frac{2\varepsilon_c}{\varepsilon_0} - (\frac{\varepsilon}{\varepsilon_0})^2\right]$$

Fig. 6 Hognestad's concrete model

Fig. 7 Comparison between $\tau_{aver,\,u}$ and $\tau_{aver\;resist}$

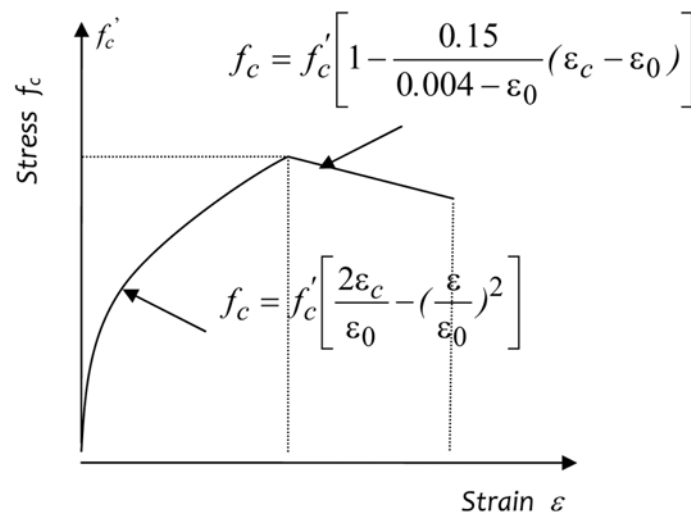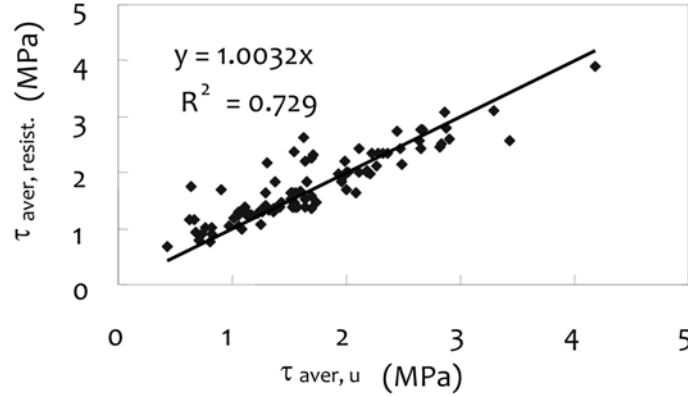the two values is good. The degree of scatter reflects the large scatter of bond strength of the FRP/concrete (Ueda and Dai 2005). As discussed in the previous section, the average bond stress in the FRP/concrete interface increases with the steel yielding length and reaches a threshold value at the ultimate state. Through the current analysis and comparison, it appears that this threshold value can be predicted using the presented bond model (Eq. 9). Therefore, a criterion is proposed in Fig. 3 to predict the maximum steel yielding length corresponding to the IC debonding limit state. Since the average bond stress driven by the steel yielding zone increases while the average bond stress resistance decreases with the increase of steel yielding length, there is a point where the values are coincident indicating the occurrence of macro debonding (see Fig. 3). In other words, the debonding criterion can be formulated as follows:

$$\tau_{aver,u} \;=\; \tau_{aver,resist.}(L_{y,u}) \tag{11}$$

If the two curves never intersect, concrete crushing will occur instead of IC debonding (see Fig. 3). The proposed criterion indicates that the occurrence of IC debonding can be attributed to the formulation of a critical debonding zone, where the tensile stress gradient of the FRP reaches its threshold value. For FRP-strengthened RC beams with steel yielding, the critical bond length is equivalent to the steel yielding length at the ultimate state. Moreover, the threshold gradient of tensile stress in the FRP proves to be equivalent in flexural tests of FRP-strengthened RC beams and simple shear tests of FRP/concrete joints. Therefore, for FRP strengthened-RC members with flexural yielding, the existence of multiple cracks seems not to have a significant influence on the critical tensile force gradient of the FRP although it does affect the maximum tensile force in FRP.

Theoretically, it should be also noticed that FRP debonding from a concrete flexural member subject to a moment gradient does not, however, result in a simple shear (Mode II) loading condition in spite of the good correlation between $\tau_{aver,\,u}$ and $\tau_{aver,\,resist}$. The moment gradient accompanying the shear introduces a component of peeling (Mode I) deformation and stress at the location of the concrete crack. This is the reason that debonding initiates at a crack and always propagates in the direction of decreasing moment. At this moment, very limited data (Wan *et al*. 2004, Dai *et al*. 2007, Pan and Lueng 2007) is available with regard to mixed-mode debonding behavior with most models preferring to address this issue empirically. The currently proposed length of the steel yielding region relative to the shear span reflects the moment gradient and thus may stand surrogate for mixed mode debonding behavior.
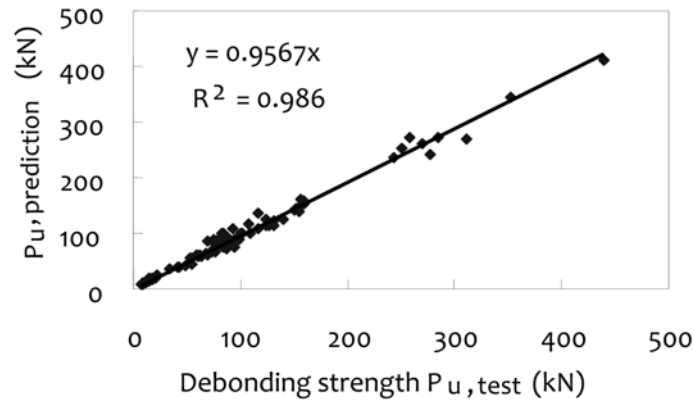
Fig. 8 Comparison between predicted and experimental load-carrying capacity

For FRP-strengthened RC beams without steel yielding or FRP-strengthened plain concrete beams, the overall gradient of tensile force in the FRP can be treated as a constant value (see Fig. 3). Therefore once the average bond stress in the FRP/concrete interface within any critical bond length reaches the threshold value, IC debonding will occur. However, the issue of determining the critical bond length remains for further study. Smith and Gravina (2007) proposed a critical bond length equal to one or two times the effective length of FRP/concrete joints under simple shear tests. The reliability of this definition must be verified based on additional experimental data since there are very few test data available for FRP-strengthened RC beams without steel yielding or for FRP-strengthened plain concrete beams with multiple cracks. On the other hand, both cases rarely appear in a design practice.

Fig. 8 presents comparisons between analytical and experimental results in terms of ultimate loading carrying capacity. The ratios of predicted load carrying capacity to experimentally observed capacity are also summarized in Table 2. The maximum, minimum, and average ratios of predicted debonding strengths to experimental capacity are 1.22, 0.81, and 0.99, respectively, and the coefficient of variation is 0.1, indicating the validity of the proposed IC debonding criterion. Comparatively, the prediction of the threshold average bond stress within the steel yielding zone (see Fig. 7) shows much greater scatter. The maximum, minimum, and average ratios of predicted threshold average bond stresses to the test results are 2.73, 0.75, and 1.09, respectively (see Table 2). The coefficient of variation is as large as 0.28. This contradiction is understandable since the member strength at debonding reflects not only the tensile force contributed by FRP through the interface bond, but also the tensile force contributed by the internal reinforcement.

6. Conclusions

Steel yielding is an important mechanism influencing the IC debonding in FRP-strengthened RC members. A simple criterion has been proposed for predicting IC debonding failure in FRP-strengthened flexural RC members having steel yielding, which is required in an appropriate ultimate state design. In this criterion, IC debonding has been attributed to the formulation of a threshold gradient of tensile force in the FRP within a critical bond zone rather than an arbitrary tensile force in FRP. The critical bond zone proves to be equivalent to the length of steel yielding in FRP-strengthened flexural RC members having steel yielding. Based on analysis of a database including 97 tests, the threshold

Table 2 Summary of analytical results of selected FRP strengthened beams/slabs

Reference	Specimen identification	a/d	$\rho s(\%)$	$E_{frp}A_{frp}/E_sA_s$	$\tau_{aver., u}$ (MPa)			Pu (kN)			Ly (mm)		
					Exp.	Pre.	Pre./	Exp.	Pre.	Pre./Exp.	Exp.	Pre.	Pre./Exp.
Beber *et al.* (1999)	VR5	3.1	0.52	0.39	2.01	2.00	1.00	102.2	100.5	0.98	254	245	0.96
	VR6	3.1	0.52	0.39	2.01	2.00	1.00	100.6	100.5	1.00	246	245	1.00
	VR7	3.1	0.52	0.68	2.65	2.77	1.05	124.2	124.6*	1.00	228	230	1.01
	VR8	3.1	0.52	0.68	2.66	2.77	1.04	124.0	124.6*	1.00	227	230	1.01
Chan and Li (2000)	B2	3.4	0.53	0.26	2.19	2.01	0.92	285.0	271.0	0.95	428	368	0.86
	B3	3.4	0.80	0.17	2.64	2.58	0.98	352.0	343.6	0.98	315	284	0.90
	B6	3.4	0.53	0.26	2.12	2.01	0.95	258.0	271.0	1.05	306	368	1.20
	B8	3.4	1.07	0.13	3.29	3.10	0.94	440.0	410.8	0.93	323	232	0.72
Dai *et al.* (2005a)	SP-C1	3.8	0.67	0.15	1.06	1.05	0.99	78.3	79.4	1.01	288	294	1.02
	SP-C2	3.8	0.67	0.30	1.57	1.37	0.87	109.0	100.9	0.93	351	319	0.91
	SP-C3	3.8	0.67	0.44	1.53	1.64	1.07	108.0	117.2	1.09	290	326	1.12
Delaney (2006)	R_UC_Control	4.1	0.89	0.21	1.55	1.63	1.05	88.8	89.0	1.00	263	265	1.01
	R_UC_Control	4.1	0.89	0.21	1.52	1.63	1.07	99.0	89.0	0.90	321	265	0.83
Garden *et al.* (1998)	3U1.0m	3.4	0.85	0.33	2.86	3.09	1.08	34.0	36.1	1.06	139	151	1.09
	1U4.5m	6.6	0.68	0.27	1.70	1.35	0.80	60.0	57.9	0.97	483	445	0.92
	4U	5.9	0.85	0.34	1.70	2.25	1.33	15.4	13.3	0.87	283	217	0.77
	5U	7.7	0.85	0.34	0.64	1.74	2.73	11.3	10.1	0.89	407	282	0.69
Kishi *et al.* (1998)	A200-1	4.2	1.07	0.03	0.67	1.15	1.72	74.0	66.5	0.90	296	172	0.58
	A200-2	4.2	1.07	0.03	0.63	1.15	1.83	76.0	66.5	0.88	315	172	0.54
	A415-1	4.2	1.07	0.06	1.05	1.29	1.23	83.4	73.8	0.88	351	220	0.63
	A623-1	4.2	1.07	0.09	1.38	1.38	1.00	79.0	79.4	1.01	248	252	1.02
	A623-2	4.2	1.07	0.09	1.42	1.38	0.97	80.5	79.4	0.99	263	252	0.96
	C300-1	4.2	1.07	0.03	0.43	0.67	1.57	79.2	89.2	1.13	217	324	1.49
	C300-2	4.2	1.07	0.06	0.73	0.90	1.24	75.0	89.2	1.19	171	324	1.90
	C445-1	4.2	1.07	0.09	0.82	1.03	1.26	84.0	100.9	1.20	208	349	1.68
	C445-2	4.2	1.07	0.09	0.77	1.03	1.33	82.8	100.9	1.22	195	349	1.79
Kishi *et al.* (2003)	A-250-1	4.2	1.07	0.05	1.32	1.32	1.00	84.2	78.0	0.93	276	213	0.77
	A-400-2	2.6	0.67	0.10	0.91	1.70	1.87	160.0	151.6	0.95	276	233	0.84
Kotynia (2005)	BF-04/0.5S	5.0	0.35	0.26	1.96	1.89	0.96	48.0	41.2	0.86	531	372	0.70
	BF-06/S	5.0	0.50	0.37	2.00	1.70	0.85	86.0	75.3	0.88	546	411	0.75
	B-08/M	4.7	0.75	0.50	2.21	1.98	0.90	140.0	125.5	0.90	538	438	0.81
	B-08/S2	4.7	0.75	0.14	3.43	2.58	0.75	94.0	75.8	0.81	483	267	0.55
	B-083m	4.7	0.75	0.13	1.11	1.38	1.24	92.0	85.6	0.93	460	289	0.63
Kurihashi *et al.* (2000)	B0-C	4.4	0.71	0.06	1.02	1.18	1.16	55.1	44.9	0.81	405	247	0.61
	R7-2	5.8	1.07	0.11	1.24	1.07	0.86	69.9	62.0	0.89	501	381	0.76
	R5-2	4.2	1.07	0.11	1.65	1.85	1.12	93.0	107.1	1.15	337	220	0.65
	R4-2	3.4	1.07	0.11	2.10	2.42	1.15	117.2	137.2	1.17	274	166	0.61
	R3-2	2.6	1.07	0.11	1.55	2.36	1.53	155.1	138.4	0.89	222	171	0.77
Rahimi and Hutchinson (2001)	B3	5.0	0.52	0.23	1.36	1.33	0.98	55.2	54.8	0.99	271	268	0.99
	B4	5.0	0.52	0.23	1.25	1.33	1.06	52.5	54.8	1.04	246	268	1.09
	B5	5.0	0.52	0.69	1.71	2.31	1.35	69.7	85.2	1.22	158	265	1.68
	B6	5.0	0.52	0.69	1.70	2.31	1.36	69.6	85.2	1.22	157	265	1.69
	B7	5.0	0.52	0.29	1.42	1.47	1.03	59.1	59.9	1.01	266	273	1.03
	B8	5.0	0.52	0.29	1.55	1.47	0.95	61.6	59.9	0.97	286	273	0.96
Saadat-	B	4.4	1.09	0.17	1.94	1.94	1.00	250.0	251.4	1.01	369	377	1.02

Table 2 Summary of analytical results of selected FRP strengthened beams/slabs

Seim *et al.* (2001)	S11	10.0	0.44	0.54	2.22	2.34	1.05	40.8	39.9	0.98	301	318	1.06
	S12	10.0	0.44	0.54	2.31	2.34	1.01	42.5	39.9	0.94	329	318	0.97
	S5	10.0	0.44	0.54	2.36	2.34	0.99	43.2	39.9	0.92	340	318	0.93
	S1m	10.0	0.44	0.54	2.27	2.34	1.03	41.9	39.9	0.95	319	318	1.00
Spadea *et al.* (2001)	A.1.1	6.0	0.96	0.18	2.08	1.64	0.79	86.8	72.0	0.83	627	394	0.63
	A.1.2	6.0	0.96	0.18	1.29	1.65	1.28	74.8	73.6	0.98	554	393	0.71
	F2	2.3	0.96	0.13	2.26	2.13	0.94	244.0	236.6	0.97	212	205	0.97
	F3	2.3	0.96	0.20	2.47	2.43	0.98	270.0	261.9	0.97	233	218	0.94
	F5	2.3	0.96	0.13	2.49	2.16	0.87	278.0	241.7	0.87	272	208	0.76
	F6	2.3	0.96	0.20	2.82	2.46	0.87	311.0	269.8	0.87	285	222	0.78
Takeo *et al.* (1999)	F1	3.8	0.64	0.10	1.08	0.99	0.91	67.7	65.2	0.96	307	306	0.99
	F1	3.1	0.64	0.10	1.14	1.22	1.07	76.7	81.5	1.06	210	247	1.18
	F1	2.7	0.64	0.10	1.31	1.37	1.05	87.0	94.2	1.08	180	220	1.22
	F1	2.1	0.64	0.10	1.96	1.83	0.93	132.0	121.4	0.92	200	169	0.85
	F1	3.8	0.64	0.20	1.16	1.24	1.07	78.6	80.7	1.03	358	353	0.99
	F1	3.8	0.64	0.30	1.30	1.42	1.10	85.6	93.4	1.09	320	376	1.18
Yao *et al.* (2005)	GS1	6.6	0.34	0.07	0.80	0.76	0.95	10.0	11.0	1.10	303	314	1.04
	GS2	6.6	0.34	0.07	0.70	0.80	1.13	9.0	10.0	1.12	256	332	1.30
	CS1	6.6	0.34	0.07	1.23	1.27	1.04	8.5	9.0	1.05	206	244	1.19
	CS2	6.6	0.35	0.07	1.51	1.52	1.01	8.8	9.4	1.06	182	231	1.27
	CP1	6.6	0.69	0.15	2.88	2.80	0.97	20.0	19.6	0.98	253	232	0.92
	CP2	6.6	0.68	0.15	2.44	2.75	1.13	17.6	19.9	1.13	153	249	1.62
	CP3	6.7	0.35	0.30	2.17	2.03	0.94	13.3	12.7	0.95	331	297	0.90
	CP4	6.7	0.34	0.30	1.99	2.21	1.11	13.5	14.8	1.10	256	322	1.26
	II-1	6.5	0.34	0.04	1.93	1.98	1.03	7.2	8.1	1.12	56	155	2.79
	II-2	6.7	0.35	0.06	1.27	1.30	1.03	8.4	8.7	1.04	208	237	1.14
	II-3	6.7	0.34	0.09	0.98	1.05	1.07	8.9	10.1	1.13	202	301	1.49
	II-4	6.7	0.35	0.12	0.82	0.90	1.10	10.2	11.0	1.07	291	339	1.16
	II-8	6.6	0.51	0.06	1.14	1.27	1.11	8.4	9.1	1.08	185	242	1.31
	II-9	6.6	0.33	0.04	1.74	1.47	0.85	6.9	7.6	1.10	72	206	2.84
	III-1	6.5	0.50	0.06	1.06	1.24	1.18	15.0	18.2	1.21	80	245	3.06
	III-2	6.4	0.50	0.13	0.68	0.94	1.37	21.4	24.7	1.15	229	322	1.41
	III-4	6.5	0.68	0.07	1.37	1.30	0.95	18.4	17.9	0.97	255	233	0.91
Zarnic *et al.* (1999)	1	3.2	0.57	0.13	4.18	3.89	0.93	116.8	108.8	0.93	196	140	0.71
	2	8.0	0.35	0.26	2.90	2.59	0.89	63.0	57.5	0.91	302	239	0.79
Zhang *et al.* (2005)	A-1	3.5	0.79	0.10	1.56	1.37	0.88	126.7	112.9	0.89	391	291	0.74
	A-2	3.5	0.79	0.10	1.56	1.37	0.88	127.0	112.9	0.89	393	291	0.74
	A-3	3.5	0.79	0.10	1.54	1.37	0.89	126.2	112.9	0.89	388	291	0.75
	A-4	3.5	0.79	0.10	1.64	1.37	0.84	131.6	112.9	0.86	421	291	0.69
	A-5	3.5	0.79	0.10	1.52	1.37	0.90	124.3	112.9	0.91	376	291	0.78
	A-6	3.5	0.79	0.10	1.57	1.37	0.87	127.2	112.9	0.89	394	291	0.74
	B-2	4.2	1.07	0.06	1.36	1.35	0.99	80.9	80.0	0.99	230	223	0.97
	B-3	4.2	1.07	0.10	1.38	1.84	1.34	84.2	78.6	0.93	269	214	0.79
	B-4	4.2	1.07	0.13	1.30	2.18	1.67	82.1	77.3	0.94	256	207	0.81
	B-6	2.6	0.67	0.12	1.60	1.68	1.05	156.3	160.5	1.03	233	254	1.09
	B-7	2.6	0.67	0.20	1.64	2.20	1.34	159.2	157.7	0.99	259	251	0.97
	B-8	2.6	0.67	0.27	1.63	2.63	1.62	156.2	151.0	0.97	254	239	0.94

Table 2 Summary of analytical results of selected FRP strengthened beams/slabs (Continued)

Zhang *et al.* (2005)	C-1	2.8	1.14	0.10	2.84	2.53	0.89	149.9	140.3	0.94	187	156	0.83
	C-2	2.6	1.07	0.10	2.65	2.44	0.92	151.9	144.9	0.95	184	162	0.88
	C-4	4.5	1.14	0.10	1.69	1.58	0.93	90.5	86.9	0.96	283	253	0.89
	C-5	4.2	1.07	0.10	1.64	1.53	0.93	94.4	89.7	0.95	300	261	0.87
	C-6	3.9	0.99	0.10	1.55	1.43	0.93	97.0	92.3	0.95	316	278	0.88
Maximum		10.0	1.14	0.69	4.18	3.89	2.73	440.0	410.8	1.22	445	627	3.06
Minimum		2.1	0.33	0.03	0.43	0.67	0.75	6.9	7.6	0.81	140	56	0.54
Mean value		4.7	0.73	0.20	1.69	1.75	1.09	96.2	93.1	0.99	270	289	1.03
C.O.V.		1.8	0.26	0.16	0.69	0.61	0.28	79.6	75.2	0.10	66	106	0.44

*compressive failure before debonding predicted in the analysis.

gradient of tensile force in FRP within the critical bond zone proves to be equivalent in flexural tests of FRP-strengthened RC beams and in simple shear tests of FRP/concrete joints. The proposed IC debonding criterion is believed to be a simple but useful tool to incorporate the effects of beam geometry, internal reinforcing and external strengthening information, and the bond properties of FRP/concrete interfaces in an IC debonding analysis. Each parameter used has clear physical meaning. Moreover, complex bond stress -slip analyses can be avoided since a conventional compatibility analysis based on the plane sections assumption is applicable for the analysis.

References

ACI 440.2R-02 (2002), "Guide for the design and construction of externally bonded FRP systems for strengthening concrete structures." American Concrete Institute, Farmington Hills MI.

Achintha, P. M. M. and Burgoyne, C. J. (2006), "A fracture-mechanics model for debonding of external fibre reinforced polymer plates on reinforced concrete beams." *Proceedings of 10th East Asia-Pacific Conference on Structural Engineering and Construction*, Vol. 6, Bangkok, Thailand, 731-736.

Arduini, M., Di Tommaso, A. and Nanni, A. (1997), "Brittle failure in FRP plate and sheet bonded beams." *ACI Struct. J.,* 94(4), 363-370.

Beber, A. J., Campos Filho, A. and Campagnolo, J. L. (1999), "Flexural strengthening of R/C beams with CFRP sheets." *Proceedings of 8th International Structural Faults and Repair Conference*, London.

Brosens, K. and Van Gemert, D. (1998), "Plate end shear design for external CFRP laminates", *Proceedings of FRAMCOS-3*, Aedificatio Publishers, Freiburg, Germany, 1793-1804.

Buyukozturk O. and Hearing B. (1998), "Fracture behavior of precracked concrete beams retrofitting with FRP." *ASCE J. Compos. Constr.,* 2(3), 138-144.

Ceroni, F., Pecce, M. and Matthys, S. (2004), "Tension stiffening of reinforced concrete ties strengthened with externally bonded fiber reinforced polymer sheets." *ASCE, J. Compos. Constr.,* 8(1), 22-32.

Chan, T. K. and Li, X. A. (2000), "Improving crack behavior of one-way slabs with carbon fibre plates." *Proceedings of the 4th Asia Pacific Structural Engineering & Construction Conference*, Kuala Lumpur, Malaysia, 351-358.

Chen, J.F., Yuan, H. and Teng, J. G. (2005), "Analysis of debonding failure along a softening FRP-to-concrete interface between two adjacent cracks." *Bond Behaviour of FRP in Structures: Proceedings of the International Symposium BBFS 2005,* Hong Kong, 103-112.

Chen, J.F., Yang, Z.J. and Holt, G.D. (2001), "FRP or steel plate-to-concrete bonded joints: Effect of test methods on experimental bond strength." *Steel & Composite Structures*, 1(2), 231-244.

Dai, J. G., Ueda, T., Sato, Y. and Ito, Y. (2005a), "Flexural strengthening of RC beams using externally bonded FRP sheets through flexible adhesive bonding." *Bond Behaviour of FRP in Structures: Proceedings of the*

International Symposium BBFS 2005, Hong Kong, 213-222.

Dai, J. G., Ueda, T. and Sato, Y. (2005b), "Development of nonlinear bond stress-slip model of FRP sheet-concrete interfaces with a simple method." *ASCE Journal of Composites for Construction,* 9(1), 52-62.

Dai, J. G., Ueda, T. and Sato, Y. (2006), "Unified analytical approaches for determining shear bond characteristics of FRP-concrete interfaces through pullout tests." *Journal of Advanced Concrete Technology,* 4(1), 133-145.

Dai, J.G., Yokota, H., Ueda, T. and Wan B. (2007), "Influence of bending and dowel action on the interface bond in RC beams strengthened with FRP sheets: An experimental investigation." Fracture Mechanics of Concrete and Concrete Structures, Vols 1-3- Vol 1: New Trends in Fracture Mechanics of Concrete; Vol 2: Design, Assessment and Retrofitting of RC Structures; Vol 3: High-Performance Concrete, Brick-Masonry and Environmental Aspects, 1149-1156.

Delaney, J. (2006), "Defect criticality of FRP rehabilitated RC beams." Master's thesis, University of California, San Diego.

FIB. (2001), "Externally bonded FRP reinforcement for RC structures." Bulletin 14, Lausanne, Switzerland.

Garden, H. N., Quantrill, R. J., Hollaway, L. C., Thorne, A. M. and Parke, G. A.R. (1997), "A preliminary evaluation of carbon fiber reinforced polymer plates for strengthening reinforced concrete members." *Proc. Inst. Civ. Eng., Struct. Build.,* 122(2), 127-142.

Garden, H. N., Quantrill, R. J., Hollaway, L. C., Thorne, A. M. and Parke, G. A. R. (1998), "An experimental study of the anchorage length of carbon fiber composite plates used to strengthen reinforced concrete beams." *Constru. Building. Mater.,* 12, 203-219.

Gunes et al. (2006), "Design of FRP retrofitted flexural members against debonding failures." *Proceedings of the 8th U.S. National Conference on Earthquake Engineering*, San Francisco, California, USA, Paper No. 1205.

Holzenkämfer, O. (1994), "*Ingenieurmodelle des Verbundes geklebter Bewehrung für Betonbauteile.*" Ph.D. Dissertation, TU Braunschweig, Germany (in German).

Ibars, E. O. (2005), "*Peeling failure in beams strengthened by plate bonding: A design proposal.*", Ph.D dissertation, Department d'Enginyeria de la Construcció, Universitat Politècnica de Catalunya, Spain.

JSCE (2001), "Recommendations for upgrading of concrete structures with use of continuous fiber sheets." *Concrete Engineering Series 41*, Japan Society of Civil Engineers.

Kim, S. H. and Aboutaha, R. S (2004), "Ductility of carbon fiber-reinforced polymer (CFRP) strengthened reinforced concrete beams: experimental investigation." *Steel & Composite Structures*, 4(5), 333-353.

Kishi, N., Mikami, H., Sato, M. and Matsoka, K. (1998), "Flexural bond behavior of RC beams externally bonded with FRP sheets." *Proceedings of the Japan Concrete Institute,* 20(1), 515-520.

Kishi, N., Mikami, H. and Zhang, G. (2003), "Numerical analysis of debonding behavior of FRP sheet for flexural strengthening RC beams." *JSCE Journal of Materials, Concrete Structures and Pavements*, 58(725), 255-272.

Kotynia, R. (2005), "Debonding failures of RC beams strengthened with externally bonded strips." *Bond Behaviour of FRP in Structures: Proceedings of the International Symposium BBFS 2005*, Hong Kong 247-252.

Kurihashi, Y., Kishi, N., Mikami, H. amd Matsoka, K. (2000), "Effect of FRP reinforcement amount on flexural bond behavior of FRP-strengthened RC beams." *Proceedings of the Japan Concrete Institute*, 22(1), 481-486.

Leung, Christhopher K. Y. (2001), "Delamination failure in concrete beams retrofitted with a bonded plate." *ASCE Journal of Materials in Civil Engineering*, 13(2), 106-113.

Leung, Christopher K. Y., Ng., Mandy Y. M. and Luk, Herman, C. Y. (2006), "Empirical approach for determining ultimate FRP strain in FRP-strengthened concrete beam." *ASCE Journal of Composites for Construction,* 10(2), 125-136.

Leung Christopher K. Y. and Tung, W. K. (2006), ''Three-parameter model for debonding of FRP plate from concrete substrate'', *ASCE Journal of Engineering Mechanics*, 132(5), 509-518.

Liu, I.S.T., Oehlers, D.J. and Seracino, R. (2007), "Study of intermediate crack debonding in adhesively plated beams." *ASCE J. Composites for Construction.,* 11(2), 175-183.

Lu, X. Z., Teng, J.G., Ye, L.P. and Jiang, J. J. (2007), "Intermediate crack debonding in FRP-strengthened beams: FE analysis and strength model." *ASCE Journal of Composites for Construction,* 11(2), 161-174.

Meier, U. (1995), "Strengthening of structures using carbon fib/epoxy composites." *Construction and Building*

Materials, **9**(6), 341-351.

Niedermeier R. (2000), "Zugkraftdeckung bei klebearmierten bauteilen (Envelope line of tensile forces while using externally bonded reinforcement)." Ph.D. Dissertation, TU Munchen (in German)

Niu, H. and Wu, Z. S. (2001), "Interfacial debonding mechanism influenced by flexural cracks in FRP-strengthened beams." *Journal of Structural Engineering, JSCE,* 47A, 1277-1288.

Niu, H. and Wu, Z. S. (2002), "Strengthening effects of RC flexural members with FRP sheets affected by adhesive layers." *Journal of Applied Mechanics,* 5, 887-897.

Niu, H. D. and Wu, Z. S. (2006), "Numerical analysis of debonding mechanisms of FRP-strengthened reinforced concrete beams." *Computer-aided civil and infrastructure engineering,* 20(5), 354-3687.

Oehlers, D.J. (2005), "Generic Debonding Mechanisms in FRP Plated Beams and Slabs." *Bond Behaviour of FRP in Structures: Proceedings of the International Symposium BBFS 2005.* Hong Kong, 35-44.

Pan, J. L. and Leung, C. K. Y. (2005), "FRP debonding under the presence of multiple cracks along a concrete beam." *Bond Behaviour of FRP in Structures: Proceedings of the International Symposium BBFS 2005,* Hong Kong, 299-304.

Pan, J.L. and Leung, Christopher K.Y. (2007), ''Debonding along the FRP–concrete interface under combined pulling/peeling effects." *Engineering Fracture Mechanics,* 74(1-2), 132-150.

Rahimi, H. and Hutchinson, A. (2001), "Concrete beams strengthened with externally bonded FRP plates", *ASCE Journal of Composites for Construction,* 5(1), 44-56.

Saadatmanesh, H. and Ehsani, M. R. (1991), "RC beams strengthened with GFRP plates. I: Experimental study." *ASCE Journal of Structural Engineering,* 117 (11), 3417-3433.

Sebastian W. M. (2001), "Significance of midspan debonding failure in FRP-plated concrete beams." *ASCE Journal of Structural Engineering,* 127(7), 792-798.

Seim, W., Hörmann, M., Karbhari, V. and Seible, F. (2001), "External FRP post strengthening of scaled concrete slabs." *ASCE Journal of Composites for Construction,* 5(2), 67-75.

Spadea, G., Swamy, R. N. and Bencardino, F. (2001), "Strength and ductility of RC beams repaired with bonded CFRP laminates." *ASCE Journal of Bridge Engineering,* 6(5), 345-355.

Smith, S.T. and Gravina, R. J. (2005), "Critical debonding length in FRP flexurally strengthened RC Beams." *Bond Behaviour of FRP in Structures: Proceedings of the International Symposium BBFS 2005,* Hong Kong, 277-282.

Smith, S.T. and Gravina, R.J. (2007), "Modeling debonding failure in FRP flexurally strengthened RC members using a local deformation model." *ASCE Journal of Composites for Construction,* 11(2), 184-191.

Täljsten, B. (1996), "Strengthening of concrete prism using the plate-bonding technique." *International Journal of Fracture,* 81, 253-266.

Takeo, K., Matsushita, H., Sagawa, Y. and Ushigome, T. (1999), "Experiment of RC beam reinforced with CFRP adhesive method having variety of shear-span ratio." *Proceedings of the Japan Concrete Institute,* 21(2), 205-210.

Teng, J. G., Chen, J. F., Smith, S. T. and Lam, L. (2002), "*FRP Strengthened RC Structures*", Wiley, West Sussex, U.K.

Teng, J. G., Smith, S. T., Yao, J. and Chen, J. F. (2003), "Intermediate crack-induced debonding in RC beams and slabs." *Construction and Building Materials,* **17**(6-7), 447-462.

Teng, J. G., Yuan, H. and Chen, J. F. (2006); "FRP-to-concrete interfaces between two adjacent cracks : Theoretical model for debonding failure." *International Journal of Solids and Structures,* 43(18-19), 5750-5778.

Triantafillou, R. C. and Plevris, N. (1992), "Strengthening of RC beams with epoxy-bonded fiber-composite materials." *Material and Structures,* 25, 201-211.

Triantafillou T. C. (1999), "*Guidelines for the Dimensioning of Reinforced Concrete Elements Strengthened with Sika Carbondur/Sikawrap.*" University of Patras, Greece.

Ueda, T., Yamaguchi, R., Shoji, K. and Sato, Y. (2002), "Study on behavior in tension of reinforced concrete members strengthened by carbon fiber sheet." *ASCE J. Composites for Construction,* 6(3), 168-174.

Ueda, T. and Dai, J. (2005), "Mode II fracture energy of FRP-concrete interfaces: its evaluation and roles in interface modeling and anchorage design." *Proceedings of the 11th International Conference on Fracture,* Paper No.4302 (CD-ROM), Turin, Italy.

Wan, B., Sutton, M., Petrou, M.F., Harries, K.A. and Li, N. (2004), "Investigation of Bond between FRP and

Concrete Undergoing Global Mixed Mode I/II Loading." *ASCE J. Eng. Mech.* 130(12), 1467-1475.

Wang, J. (2006), "Cohesive zone model of intermediate crack-induced debonding of FRP-plated concrete beam." *International Journal of Solids and Structures,* 43(21), 6630-6648.

Wu, Z. S. and Niu, H. D. (2000), "Shear transfer along FRP-concrete interface in flexural members." *Journal of Material, Concrete Structures and Pavements",* 49(662), 231-245.

Wu, Z. S. and Niu, H. D. (2007), "Prediction of crack-induced debonding failure in R/C Structures flexurally strengthened with externally bonded FRP composites." *Doboku Gakkai Ronbunshuu E*, 63(4), 620-639.

Yao, J., Teng, J.G. and Lam, L. (2005), "Experimental study on intermediate crack debonding in FRP-Strengthened RC flexural members." *Advances in Structural Engineering,* 8(4), 365-396.

Zarniç, R., Gostic, S., Bosiljkov, V. and Bokan-Bosiljkov, V. (1999), "Improvement of bending load-bearing capacity by externally bonded plates." *Proceedings of Creating with Concrete,* Dhir and Henderson (eds), London, Thomas Telford, 433-442.

Zhang, G. F., Kishi, N., Mikami, H. and Komuro, M. (2005), "a numerical prediction method for flexural behavior of RC beams reinforced with FRP sheet." *Bond Behaviour of FRP in Structures: Proceedings of the International Symposium BBFS 2005,* Hong Kong, 215-220.

CC